The 5th International Symposium - Supercritical CO2 Power Cycles
March 28-31, 2016, San Antonio, Texas

A Compressible Hydrodynamic Analysis of Journal Bearings Lubricated with Supercritical Carbon Dioxide

Saeid Dousti
Senior Technical Fellow
Rotor Bearing Solutions International
Charlottesville, VA
Saeid.Dousti@rotorsolution.com

Paul Allaire
Chief Technical Officer
Rotor Bearing Solutions International
Charlottesville, VA
Paul.Allaire@rotorsolution.com


Saeid Dousti specializes in advanced analysis of fluid film bearings and squeeze film dampers. He has been working in this area since 2008. He obtained his Ph.D. in Mechanical and Aerospace Engineering in 2014 from the University of Virginia. Saeid has a strong background in hydrodynamic analysis and lubrication theory.


Paul is a co-founder of Rotor Bearing Solutions International. In 1980 he started the Rotating Machinery and Controls Industrial Research Lab, at the University of Virginia with several other professors and was its first Director. From 2002 to 2012, he was again the Director of ROMAC. Paul Allaire has his B. S. and M. E. degrees in Mechanical Engineering from Yale in 1963 and 1964 respectively. He taught engineering in the Telecommunications Institute in Addis Ababa Ethiopia from 1964 to 1966 while in the US Peace Corps. He got his Ph. D. degree in Mechanical Engineering from Northwestern University in 1971. Then he taught engineering at Memorial University of Newfoundland. He started in the Mechanical Engineering Department, at the University of Virginia in 1972, as an Assistant Professor. He started rotordynamic research with Edgar J. Gunter at that time. He was promoted to Associate Professor, Full Professor, Department Chair of Mechanical and Aerospace Engineering, given the Mac Wade Chaired Professor appointment, all by 1991.

ABSTRACT

Rotating power machinery associated with the advanced Brayton cycle using supercritical carbon dioxide (hereon SCO_2) as the working fluid requires well designed bearings. Certainly one of the options for this type of machinery is hydrodynamic bearings. The pressure, density relation for these bearings is complex and studies on this bearing topic have not been reported much in the literature. This paper presents a new, compressible Reynolds equation to model the lubrication in the supercritical phase in any types of high speed hydrodynamic bearings such as fixed pad or tilting pad bearings under isothermal conditions. A semi-linear new form of Reynolds equation is obtained which allows for the systematic pressure/density solution for an SCO_2 lubricated bearing. The compressible Reynolds equation solution method is then used to model a typical plain journal bearing lubricated in SCO_2 with inlet pressure of approximately 8(MPa), density of 300(kg/m^3), and viscosity of 0.1(mPa.s) at a speed of 60000(rpm). The pressure, density, and viscosity variations are evaluated for the example bearing and the results compared to an incompressible solution for the same bearing. Also, the operating shaft eccentricity ratio, attitude angle and load capacity are evaluated. It is shown that lubrication with compressible fluids can be potentially more stable. The load capacity is found to be relatively large, indicating the strong potential for use in high speed SCO_2 applications as compared to other options such as gas-foil bearings or ball bearings.

Compressible Reynolds equation, Supercritical CO_2, Hydrodynamic Lubrication

---

1. Introduction

Advanced Brayton cycle power generation devices based upon supercritical working fluids is a topic of major research today [1, 2]. These include solar, nuclear or fossil heat sources. A major focus has been on supercritical carbon dioxide (SCO_2) as the working fluid. This fluid has the potential for high efficiency in the temperature range of interest for the cited applications. The other advantages are very compact systems compared to existing systems and relatively low capital costs. Relevant rotating machines include turbines, alternator and compressors capable of operating at very high pressure densities, high rotating speeds, high pressures, and high fluid densities. The critical point for SCO_2 is

$$
\begin{aligned}
&T_{cr} = 304.1(^\circ K) = 31.1(^\circ C) = 547(^\circ R) = 88(^\circ F) \\
&P_{cr} = 7.38(MPa) = 72.8(bar) = 1070(psia) \\
&\rho_{cr} = 469(kg/m^3)
\end{aligned}
$$

Generally, the supercritical fluids are 100 to 1000 times denser than gases and slightly lighter than liquids. Also, the absolute viscosity of supercritical fluids is 5 to 10 times more viscous than gases but approximately 10 times less than liquids.

A Scandia Laboratories small scale test rig was developed for a $250(kW)$ power level involving a turbine-compressor-generator system operating at $75000(rpm)$ [1]. Gas-foil bearings were employed in the test rig but numerous design and manufacturing issues were encountered [1, 2, 3, 4, 5]. It was noted by Iverson [2] that a significant challenge for improved bearing design, among other issues, will have to be overcome before industrial use of SCO_2 power producing rotating machines can be developed.

2. Typical Pressure/Density/Viscosity Range of SCO_2 as a Lubricant

The primary purpose of this paper is to present the analysis and design of SCO_2 lubricated bearings, operating in the supercritical range. Almost no literature has been published on this topic so far. Because of the complex relations between pressure, density and viscosity, the solution is difficult. This type of bearing could potentially be used in high speed SCO_2 turbines instead of oil bearings or magnetic bearings.

A typical maximum hydrodynamic pressure generated in a small high speed SCO_2 bearing is in the range of

$$\Delta p_{max} \leq 1\text{-}2(MPa) = 10\text{-}20(bar) = 145\text{-}290(psia) \tag{1}$$

We can easily see that this value is much smaller than the critical SCO_2 pressure at $7.28(MPa)$. The typical bearing operation is approximately

$$\begin{array}{ll} 80 \text{ to } 90(bar) & \text{(Pressure Range)} \\ 480 \text{ to } 580(kg/m^3) & \text{(Density Range)} \\ 35 \text{ to } 50(^\circ C) & \text{(Temperature Range)} \end{array}$$

These are the likely operating pressure/density/temperature range for SCO_2 hydrodynamic bearings in industrial Brayton Cycle applications.

3. Gas-Foil Bearings in Sandia Use

One of the key components for this technology is the bearings used to support the rotating devices at high speeds. Early tests employed ball bearings but only limited life was obtained. Gas-foil bearings were employed later by Barber Nichols in the Sandia tests [1]. The Sandia compressor loop operated at $75000(rpm)$ due to the small nature of the test configuration. The gas-foil bearings have limited load capacity and the loads on them must be carefully evaluated to insure adequate rotor support. Also, it is difficult to start the rotors in gas-foil bearings [1]. To avoid overheating the gas-foil bearing, they are operated at reduced pressures below 300 psia. It has been noted that the development costs for the gas-foil bearing consumed a large fraction of the funds for the Sandia test rig [2]. The presence of turbulence in the tight clearance of the gas-foil bearing caused a sharp increase in the dependency of the frictional loss and load capacity in the radial and thrust gas-foil bearings to environmental conditions [2]. There was a heightened sensitivity to lubricant gas pressure and running speed. This same phenomenon was observed in the NASA Glenn Research Center when testing gas-foil bearings [3]. The gas-foil bearings for the Sandia test rig required extensive custom fabrication, iterative design and a testing process [2]. A long list of potential improvements to the gas-foil bearings includes smaller diameters, fewer thrust pads, geometric features such as chevrons at the trailing edge of each thrust pad to expel hot fluid, stamped manufacturing to reduce manufacturing costs, as well as smaller operating film thicknesses for higher load capacity and plasma spray with a solid lubricant to increase temperature resistance [2]. In other words, a major research project on gas-foil bearings would be required to make them useful for industrial applications.

4. Industrial Scale Turbomachinery for SCO2 Technology

It has been estimated that a $10(MW)$ size represents the minimum size of a commercial scale Brayton cycle machine [4]. This would be a multi-stage axial turbine with operating speed of approximately $24000(rpm)$, an operating speed much like present day industrial axial gas turbines. Such a turbine could then potentially be mated to a gearbox driving a generator at $3600(rpm)$ or $3000(rpm)$. It has also been suggested that conventional oil lubricated bearings be employed for industrial SCO_2 machines [5]. However, this will require highly effective seals to keep the most of the oil out of the SCO_2 working fluid. Also, the power loss of oil lubricated bearings means significant reductions in turbine efficiency as well as unwanted heating in the bearing areas. The viscosity of SCO_2 is much lower than that of oil so it is expected that the power loss will be much lower.

It is likely that a much more practical solution is that of SCO_2 hydrodynamic bearings. As already noted, the purpose of this paper is to develop a new, useful Reynolds equation for SCO_2 that can be used to design industrial bearings. It is estimated that the cost of these $SC0_2$ bearings will be modest compared to the costs of the alternatives such as gas-foil bearings and magnetic bearings. The next phases of this development include the design and testing of such bearings in some university or industrial test rigs.

5. A New Compressible Reynolds Equation for SCO_2 Lubrication

A new formulation of the isothermal compressible Reynolds equation applicable to SCO_2 lubricated fixed or tilting pad bearings is developed. However, the relationship between the SCO_2 pressure, density and viscosity is complicated and interdependent. The method developed in this work starts with the compressible, isothermal Reynolds equation [6] as

$$\frac{\partial}{\partial x}\left(\frac{\rho h^3}{k_x \mu}\frac{\partial p}{\partial x}\right)+\frac{\partial}{\partial z}\left(\frac{\rho h^3}{k_z \mu}\frac{\partial p}{\partial z}\right)=\rho\frac{\partial h}{\partial t}+\frac{1}{2}U\frac{\partial\left(\rho h\right)}{\partial x} \tag{2}$$

where x, z are the circumferential and axial coordinates, and U denotes journal surface velocity. In the above equation, h is the film thickness which varies in circumferential direction as

$$h = c + e\cos\theta = c\left(1+\epsilon\cos\theta\right) \tag{3}$$

where c denotes radial clearance, e stands for journal eccentricity, and ϵ is the eccentricity ratio as shown in Fig. (2). Solving Eq. (2) is very challenging due to the involvement of two unknowns of pressure and density in the gradient terms on the left hand side of the equation. In Eq. (2) turbulence is accounted for based on Constantinescu's approach using k_x, k_z coefficients defined as

$$\text{Laminar}: \qquad k_x = 12 \quad , \quad k_z = 12 \tag{4}$$

$$\text{Turbulent}: \qquad \begin{cases} k_x = 12 + 0.0136\mathbf{Re}^{0.9} \\ k_z = 12 + 0.0043\mathbf{Re}^{0.96} \end{cases} \tag{5}$$

In the turbulent regime k_x, k_z are Reynolds number dependent. The Reynolds number, which is defined as $\mathbf{Re} = \frac{\rho U c}{\mu}$, determines if the fluid is at laminar, turbulent or in the transition regime. In this study, the $500 < \mathbf{Re} < 1000$ interval is considered as the transition to turbulence regime and operations with $\mathbf{Re}$ below 500 and above 1000 are considered laminar and turbulent, respectively [7, 8, 9].

Equation (2) involves the film pressure, density, and viscosity and is highly nonlinear. It is desired to simplify the solution of the compressible Reynolds equation. A pressure parameter solution assuming an ideal gas pressure/density relation and also that the pressure parameter is the square of the pressure, p^2, is given in the literature [10]. Now, the left hand of Reynolds equation is linear in the pressure squared leading to a semi-linear form. On the right hand side, the shear and time dependent terms involve the pressure linearly or involving the square root of the pressure squared. This form of equation is suitable for an isothermal perfect gas lubrication but is still not accurate enough to model SCO_2 in use as a lubricant.

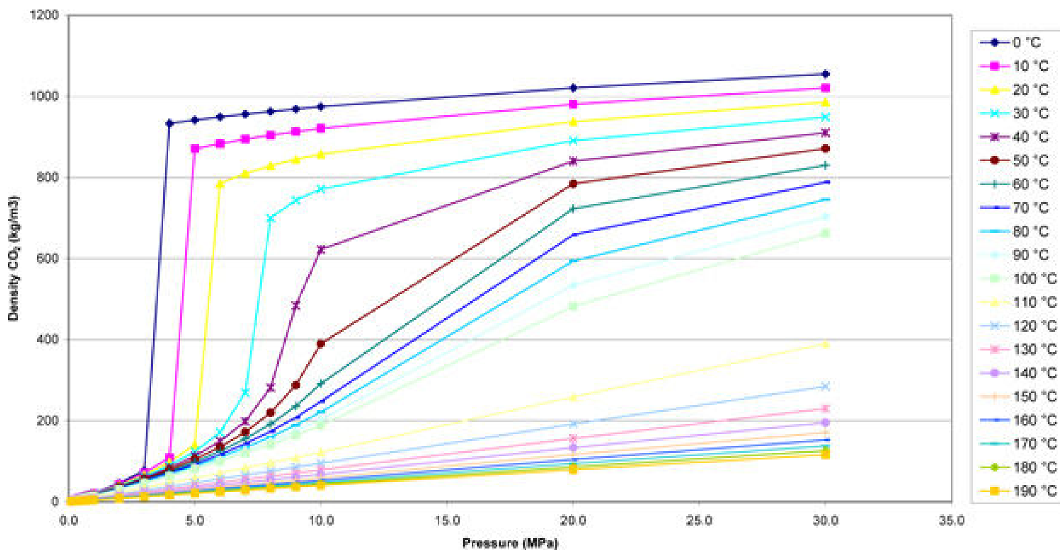

Figure 1: Density of carbon dioxide as function of the pressure for various temperatures

6. Viscosity and Density

The transport properties of SCO_2, such as viscosity and density, at the vicinity of its critical point, i.e., $T_c = 304.1(k)$ and $P_c = 7.38(MPa)$, are very sensitive to temperature and pressure changes and their behavior deviates away from ideal gas significantly. Researchers have proposed various complex models to capture these nonlinear behaviors [11, 12].

To model the very nonlinear dependence of the density on temperature and pressure, Wang, Sun, and Yan developed a six and three degree polynomial in pressure and temperature, respectively, which correlated very well with experimental data [11]. This equation is

$$\begin{aligned} \rho = & \left(a_1 T_r^3 + a_2 T_r^2 + a_3 T_r + a_4\right) p_r^6 \\ & + \left(b_1 T_r^3 + b_2 T_r^2 + b_3 T_r + b_4\right) p_r^5 \\ & + \left(c_1 T_r^3 + c_2 T_r^2 + c_3 T_r + c_4\right) p_r^4 \\ & + \left(d_1 T_r^3 + d_2 T_r^2 + d_3 T_r + d_4\right) p_r^3 \\ & + \left(e_1 T_r^3 + e_2 T_r^2 + e_3 T_r + e_4\right) p_r^2 \\ & + \left(f_1 T_r^3 + f_2 T_r^2 + f_3 T_r + f_4\right) p_r \\ & + \left(g_1 T_r^3 + g_2 T_r^2 + g_3 T_r + g_4\right) \end{aligned} \quad (6)$$

where $T_r = T/T_c$ and $p_r = p/p_c$ are the relative temperature and pressure.

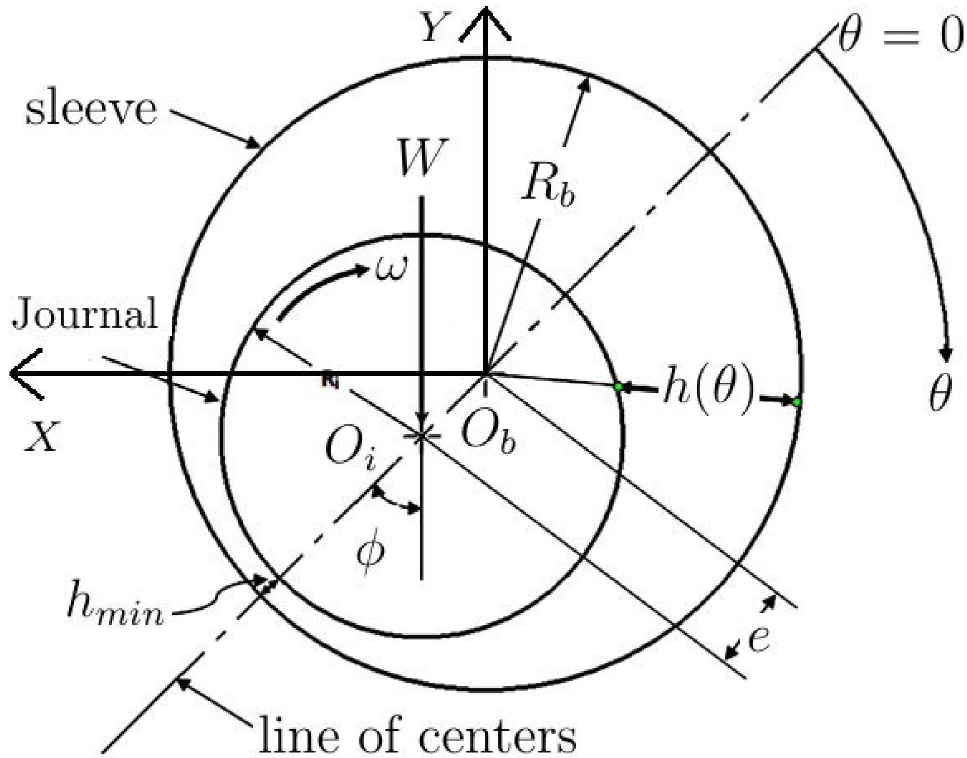

Figure 2: Journal bearing

Equation (6) is valid for the range $303(K) < T < 473(K)$ and $3(MPa) < p < 60(MPa)$[1].

The viscosity of CO_2 is studied by Fenghour and Wakeham [12]. They proposed an analytical model suggesting the dependence of viscosity on temperature and density as

$$\mu = \mu_o(T) + \Delta\mu(\rho, T) \tag{7}$$

$$\mu_o(T) = \frac{1.00697\sqrt{T}}{G(T^*)} \tag{8}$$

[1]For the constants in Eq. (6) consult reference [11]. Be noted that the correct value of the c_4 is -23259.58953 and is incorrect in the original paper.

where

$$\ln G(T^*) = \sum_{i=0}^{4} \alpha_i \left(\ln T^*\right)^i \tag{9}$$

$$T^* = \frac{kT}{\epsilon} \quad , \quad \frac{\epsilon}{k} = 251.196 \tag{10}$$

$$\Delta\mu(\rho, T) = d_{11}\rho + d_{21}\rho^2 + \frac{d_{64}\rho^6}{T^{*3}} + d_{81}\rho^8 + \frac{d_{82}\rho^8}{T^*} \tag{11}$$

where d_{ij}s are constants [12]. A combination of Eqs. (6-11) offers a nonlinear variation of density and viscosity of CO_2 with temperature and pressure specially in supercritical phase.

The viscosity of SCO_2 is between 0.01-0.1($mPa.s$) which is much less than that of the conventional oil based lubricants with a typical viscosity of 30($mPa.s$). Thus, in the lack of significant lubricant shearing in the case of SCO_2, an isothermal process of the lubricant film is a reasonable assumption.

Equation (6), by offering a relation between density and pressure, serves to reduce Eq. (2). However, Eq. (6) is yet too complicated to be readily used. As mentioned before, the hydrodynamic pressure that is generated in the bearing clearance is in general much less than the supply pressure and allows for a linearization of the density versus pressure as

$$\rho = \alpha(T)p + \rho_o \tag{12}$$

instead of using the full Eq. (6). In Fig. (1), it is shown that this linear range is variant for different temperatures and its range and slope varies.

Equation (12) allows for significant simplification of the Reynolds equation (2) to

$$\begin{aligned} &\frac{\partial}{\partial x}\left(\alpha(T)\frac{h^3}{2k_x\mu}\frac{\partial p^2}{\partial x}\right) + \frac{\partial}{\partial z}\left(\alpha(T)\frac{h^3}{2k_z\mu}\frac{\partial p^2}{\partial z}\right) = \\ &\qquad +\rho\frac{\partial h}{\partial t} + \frac{1}{2}U\frac{\partial(\rho h)}{\partial x} - \rho_o\left\{\frac{\partial}{\partial x}\left(\frac{h^3}{k_x\mu}\frac{\partial p}{\partial x}\right) + \frac{\partial}{\partial z}\left(\frac{h^3}{k_z\mu}\frac{\partial p}{\partial z}\right)\right\} \end{aligned} \tag{13}$$

where only the density in the left hand side of Eq. (2) is replaced using Eq. (12). This allows for a solution of the above equation in terms of p^2, whilst the right hand side of the equation uses the general density and viscosity equations (6-11). This feature eventually translates into an iterative nature of solution elaborated in Sec. (7). Note that Eq. (13) is different from the ideal gas Reynolds equation suggested in [10] in that, it contains a ρ_o-dependent correcting term in the right hand side. Once the pressure profile is calculated, the load carrying capacity of the bearing is calculated as

$$F_X = -\int\int p\cos\theta' dxdz \tag{14}$$

$$F_Y = -\int\int p\sin\theta' dxdz \tag{15}$$

where F_X and F_Y are the external force components and θ' is measured from the X axis shown in Fig. (2) in clockwise direction.

7. Solution Algorithm

To solve the proposed compressible Reynolds Eq. (13), a finite element based method is adopted [13]. As mentioned before, an isothermal process is a reasonable approach for the solution. The following algorithm is used

i. Use the supply pressure and temperature, p_s, T_s, which are expected to be in the order of critical values, p_c and T_c, to find $\alpha(T)$ and ρ_o based on Eq. (6) for a linear range (see Fig. 1).

ii. Initialize the solution process by assuming $p = p_s, T = T_s$ on all finite element node points and use Eqs. (6,7) to find the density and viscosity of the lubricant.

iii. Solve Eq. (13) to find p^2 and consequently p, using a standard 2-D FEA method.

iv. Update the values of ρ and μ based on newly found pressure profile using Eqs. (6,7).

v. Compare the new pressure profile with the old one for convergence. Repeat the algorithm if the pressure difference is larger than the desired threshold.

The proposed algorithm is very robust and converges in a very low number of iterations. Note that in the bearings operating close to the critical point of CO_2 cavitation phenomenon does not occur [9].

Table 1: Bearing geometry and operation conditions.

Diameter, $D(mm)$	40
Clearance ratio, c/R	0.001
Length, $L(mm)$	40
Temperature,$T(K)$	320
Supply pressure,$P_s(MPa)$	8
Supply viscosity,$\mu(\mu Pa.s)$	24.7
Supply density,$\rho(kg/m^3)$	321.051
Rotational speed, $\omega(rpm)$	60000
Bearing type	cylindrical sleeve
Supply condition	fully flooded

8. Numerical Results

A cylindrical sleeve bearing, Fig. 2, with its properties tabulated in Table 1 is analyzed here. Once the viscosity of the lubricant is very low, the bearing has to operate at relatively high speeds to compensate for the low viscosity. Thus, the rotational speed is chosen to be 60000(rpm) for this example.

The pressure solution is a function of x,z. Figure (3a) depicts the pressure profile in the middle of the axial length, $z = \frac{L}{2}$, for various journal eccentricities. As the eccentricity of the journal in the bearing housing increases, higher hydrodynamic loads are generated. A comparison is made between the results of the proposed compressible Reynolds equation and the pressure profile resulted from the incompressible Reynolds equation [14]. To this end, the normal pressure difference is defined as

$$\Delta\bar{p}\% = \frac{p_{in} - p}{p_{in}} * 100 \tag{16}$$

where p_{in} is the incompressible pressure profile which is illustrated in Fig. (3b). It is seen that for the specific operation condition listed in Table (1), the error of using an incompressible Reynolds equation is significant even for moderate eccentricity ratios.

In an isothermal incompressible analysis, viscosity and density are constant in all of the pressure domain. However, in a compressible analysis, these two parameters vary spatially, as shown in Fig. (4). In both cases, the peak values occur where the max pressure takes place. The reduction of

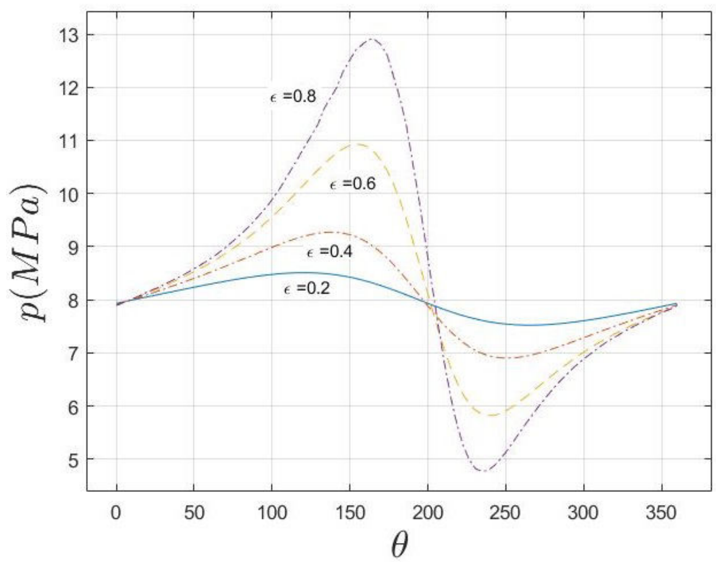

(a) circumferential pressure profile obtained from compressible analysis

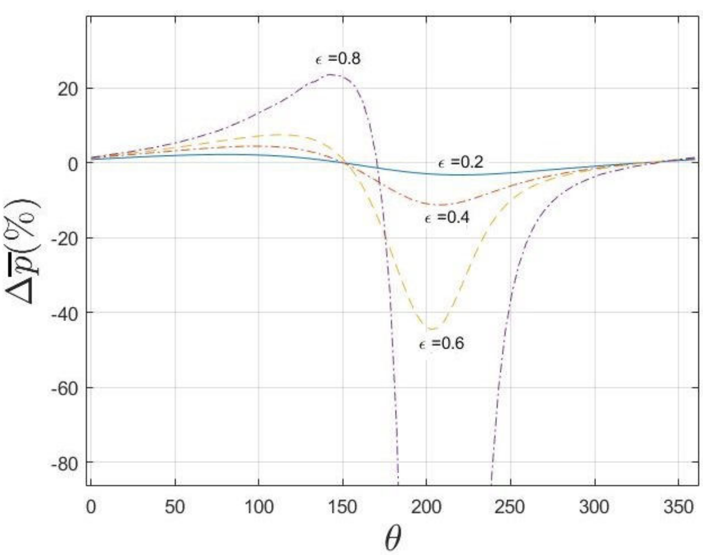

(b) normalized circumferential pressure difference between compressible and incompressible analysis

Figure 3: Circumferential pressure profile at $z = \frac{L}{2}$ obtained from the compressible analysis and its normal difference compared to the pressure profile obtained from an incompressible fluid assumption for different eccentricity ratios.

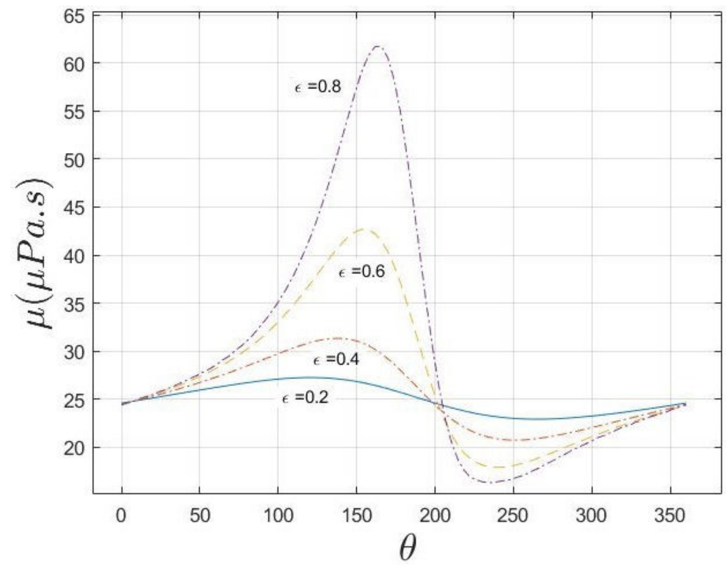

(a) circumferential viscosity profile

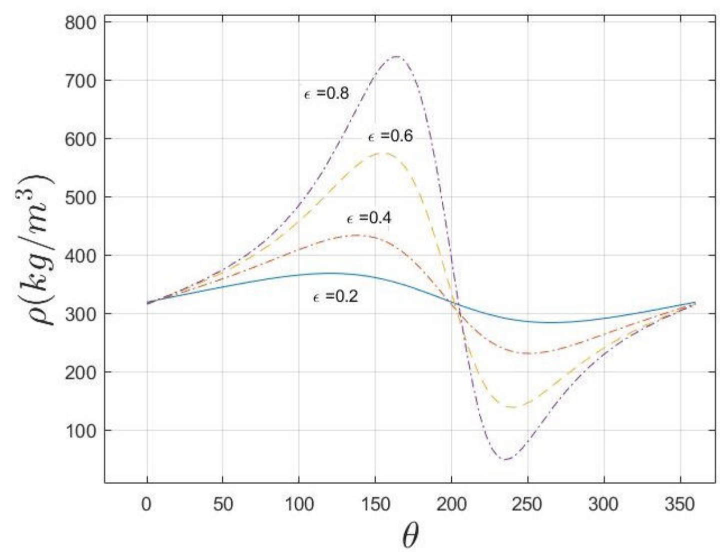

(b) circumferential density profile

Figure 4: Viscosity and density circumferential profile at $z = \frac{L}{2}$ for various eccentricity ratios.

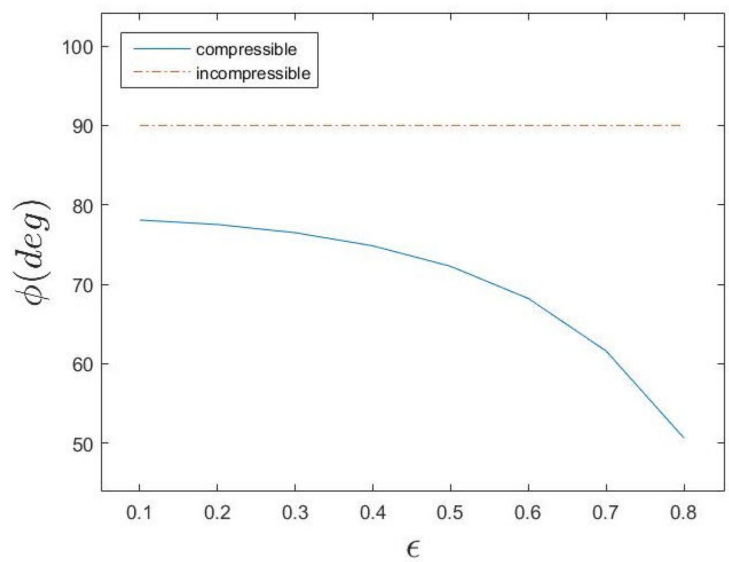

(a) attitude angle ϕ

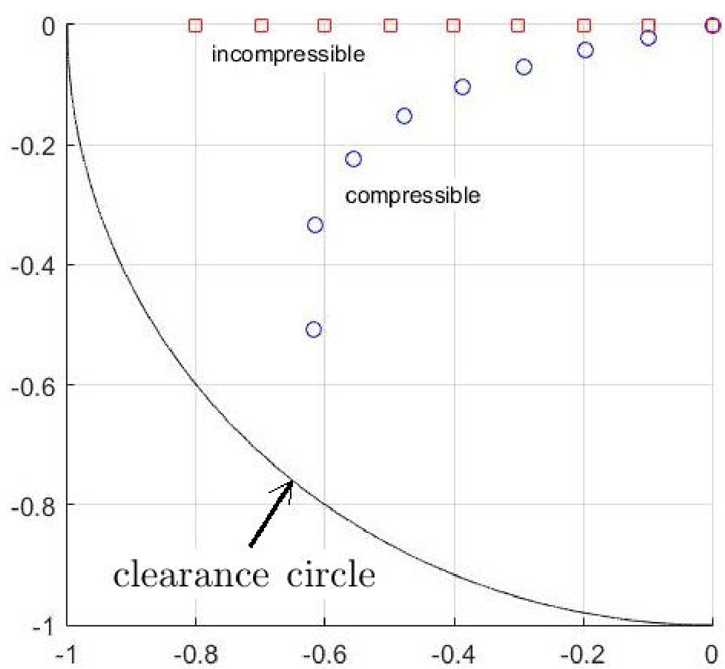

(b) journal center locus

Figure 5: Journal center position in clearance circle obtained from compressible and incompressible analysis.

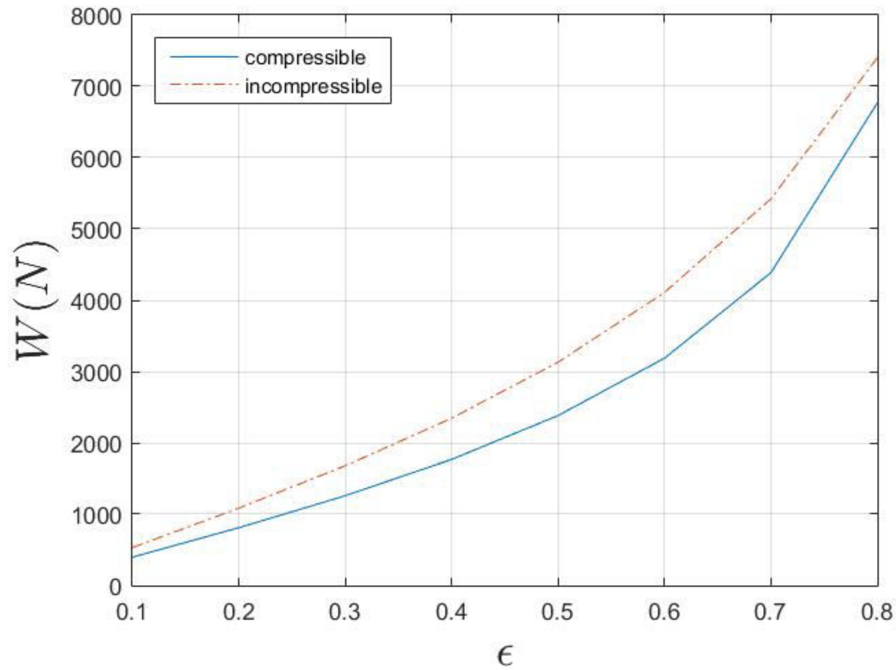

Figure 6: Load capacity of the bearing running at 60000(rpm).

the viscosity when the pressure drops below p_s is less intense compared to the density. The variation of the viscosity and the density increases as the eccentricity ratio increases.

The main difference between a compressible and an incompressible analysis occurs in the prediction of the journal position and the attitude angle. For a noncavitated cylindrical bearing, the incompressible analysis always predicts a 90(deg) angle between the external force and the journal motion [6, 10]. This phenomenon translates into high cross couple dynamic coefficients of the bearing and instability. However, a compressible analysis predicts attitude angles lower than 90(deg) which decreases as the eccentricity ratio increases. This observation may showcase and prove an advantage of using compressible lubricants over the comparable incompressible ones. This paper does not present bearing stiffness and damping coefficients. Further investigations are required on the topic of the stability if compressible process supercritical lubricated bearings.

Figure (6) depicts the load capacity of the bearing versus eccentricity. As expected, lower load capacities occur when the compressible analysis is used for all the cases. The load capacity at high speed is significant for the high speed operation of SCO_2 bearings.

8.1. Friction Power Loss

Another objective here is to estimate the power loss of a bearing lubricated with SCO_2 and compare it to a similar oil lubricated bearing. To this end, Petroff's simple formula which is based on the centered bearing is used [15]

$$T_f = \frac{4\pi^2 \mu N L R^3}{c} \quad (N.m) \tag{17}$$

$$P_f = \frac{T_f N_{rpm}}{9549} \quad (kW) \tag{18}$$

where N and N_{rpm} are the rotational speed in (rev/s) and (rpm), respectively. For the analyzed bearing in the previous section and assuming an average viscosity of $24.7(\mu Pa.s)$ for the SCO_2, we have

$$T_f = 0.0156 \quad (N.m) \tag{19}$$

$$P_f = 0.0979 \quad (kW) \tag{20}$$

while for a similar oil lubricated bearing with an average viscosity of $1(mPa.s)$ the above values are

$$T_f = 0.6316 \quad (N.m) \tag{21}$$

$$P_f = 3.9636 \quad (kW) \tag{22}$$

which is about 40 time larger. So it can be concluded that the use of SCO_2 can be advantageous in lowering the power loss at high speeds.

9. Summary and Results

In this paper, we address the problem of bearing lubricated with supercritical carbon dioxide. The results can be summarized as

i. A new compressible Reynolds equation is developed that extends the ideal gas lubrication theory to a supercritical phase.

ii. A semi-linear solution method has been developed using linear approximations for the density and viscosity. An FEA based solution is developed that is proven to be very fast and robust.

iii. A high speed cylindrical bearing lubricated with supercritical CO_2 applicable in turbogenerators used in Brayton cycles power machines, is analyzed.

iv. The numerical results show that the variation of the lubricant's density and viscosity can be considerable, specially at higher loads and eccentricities.

v. While the incompressible hydrodynamic theory predicts a $90(deg)$ attitude angles for all external loads, the developed theory results in attitude angles lower than $90(deg)$, which can translate into more stable bearings. Additionally, as expected, the incompressible Reynolds equation results in an overestimation of the bearing's load capacity.

vi. The very low viscosity of the SCO_2 allows for much smaller power losses at high speeds compared to oil lubricated bearings.

The study of tilting pad bearings lubricated with SCO_2 and their dynamic properties is the subject of future paper.

References

[1] S. A. Wright, R. F. Radel, M. E. Vernon, G. E. Rochau, P. S. Pickard, "Operation and analysis of a super"critical co2 brayton cycle, Sandia Report, No. SAND2010-0171.

[2] B. D. Iverson, T. M. Conboy, J. J. Pasch, A. M. Kruizenga, "Supercritical CO 2 Brayton cycles for solar-thermal energy", Applied Energy 111 (2013) 957–970.

[3] R. J. Bruckner, "Windage Power Loss in Gas Foil Bearings and the Rotor-Stator Clearance of High Speed Generators Operating in High Pressure Environments", in: ASME Turbo Expo 2009: Power for Land, Sea, and Air, American Society of Mechanical Engineers, 2009, pp. 263–270.

[4] J. J. Sienicki, A. Moisseytsev, R. L. Fuller, S. A. Wright, P. S. Pickard, "Scale dependencies of supercritical carbon dioxide Brayton cycle technologies and the optimal size for a next-step supercritical CO2 cycle demonstration", in: 2011 Supercritical CO2 Power Cycle Symposium, Boulder, CO, 2011.

[5] R. Fuller, "Turbo-machinery considerations using super-critical carbon dioxide working fluid for a closed Brayton cycle", in: SCO2 Power Symposium, 2007.

[6] A. Cameron, The principles of lubrication, Wiley, 1966.

[7] V. N. Constantinescu, S. Galetuse, "Operating Characteristics of Journal Bearings in Turbulent Inertial Flow", Journal of Lubrication Technology 104 (2) (1982) 173–179.

[8] V. N. Constantinescu, S. Galetuse, "On the Possibilities of Improving the Accuracy of the Evaluation of Inertia Forces in Laminar and Turbulent Films", Journal of Lubrication Technology 96 (1) (1974) 69–77. doi:10.1115/1.3451912.
URL http://dx.doi.org/10.1115/1.3451912

[9] S. Dousti, J. Cao, A. Younan, P. Allaire, T. Dimond, "Temporal and Convective Inertia Effects in Plain Journal Bearings with Eccentricity, Velocity and Acceleration", Journal of Tribology 134 (3) (2012) 505–512. doi:10.1115/1.4006928.

[10] W. A. Gross, Gas film lubrication, Wiley, 1962.

[11] Z. Wang, B. Sun, L. Yan, "Improved Density Correlation for Supercritical CO2", Chemical Engineering & Technology 38 (1) (2015) 75–84. doi:10.1002/ceat.201400357.
URL http://dx.doi.org/10.1002/ceat.201400357

[12] A. Fenghour, W. A. Wakeham, V. Vesovic, "The Viscosity of Carbon Dioxide", Journal of Physical and Chemical Reference Data 27 (1) (1998) 31–44. doi:http://dx.doi.org/10.1063/1.556013.
URL http://scitation.aip.org/content/aip/journal/jpcrd/27/1/10.1063/1.556013

[13] S. Dousti, R. Fittro, "An Extended Reynolds Equation Including The Lubricant Inertia Effects: Application to Finite Length Water Lubricated Bearings", ASME 2015 Turbo Expo, GT2015-43826, Montreal, Canada.

[14] S. Dousti, P. Allaire, T. Dimond, J. Cao, "An Extended Reynold Equation Applicable to High Reduced Reynolds Operation of Journal Bearings", Submitted to Tribology International.

[15] R. C. Juvinall, K. M. Marshek, "Fundamentals of Machine Component Design", Vol. 83, John Wiley & Sons New York, 2006.